Plant Mol Biol (2010) 74:91–103
DOI 10.1007/s11103-010-9656-x

Mutation in *Wilted Dwarf and Lethal 1* (*WDL1*) causes abnormal cuticle formation and rapid water loss in rice

Jong-Jin Park · Ping Jin · Jinmi Yoon · Jung-Il Yang · Hee Joong Jeong · Kosala Ranathunge · Lukas Schreiber · Rochus Franke · In-Jung Lee · Gynheung An

Received: 10 March 2010 / Accepted: 9 June 2010 / Published online: 30 June 2010

Abstract Epidermal cell layers play important roles in plant defenses against various environmental stresses. Here we report the identification of a cuticle membrane mutant, *wilted dwarf and lethal 1* (*wdl1*), from a rice T-DNA insertional population. The muant is dwarf and die at seedling stage due to increased rates of water loss. Stomatal cells and pavement cells are smaller in the mutant, suggesting that *WDL1* affects epidermal cell differentiation. T-DNA was inserted into a gene that encodes a protein belonging to the SGNH subfamily, within the GDSL lipase superfamily. The WDL1–sGFP signal coincided with the RFP signal driven by *AtBIP–mRFP*, indicating that WDL1 is an ER protein. SEM analyses showed that their leaves have a disorganized crystal wax layer. Cross-sectioning reveals loose packing of the cuticle and irregular thickness of cell wall. Detailed analyses of the epicuticular wax showed no significant changes either in the total amount and amounts of each monomer or in the levels of lipid polymers, including cutin and other covalently bound lipids, attached to the cell wall. We propose that *WDL1* is involved in cutin organization, affecting depolymerizable components.

Keywords Cutin · Epicuticular layer · GDSL lipase · Permeability · Rice · Wax

Electronic supplementary material The online version of this article (doi:10.1007/s11103-010-9656-x) contains supplementary material, which is available to authorized users.

J.-J. Park · P. Jin · J. Yoon · J.-I. Yang · H. J. Jeong · G. An
Department of Life Science, Pohang University of Science and Technology (POSTECH), Pohang 790-784, Republic of Korea

J.-J. Park · P. Jin · J. Yoon · J.-I. Yang · H. J. Jeong · G. An (✉)
Crop Biotech Institute and Department of Plant Molecular Systems Biotech, Kyung Hee University, Yongin 446-701, Korea
e-mail: genean@khu.ac.kr

K. Ranathunge · L. Schreiber · R. Franke
Institute of Cellular and Molecular Botany, University of Bonn, Kirschallee 1, 53115 Bonn, Germany

I.-J. Lee
Division of Plant Biosciences, College of Agriculture and Life Sciences, Kyungpook National University, Daegu 702-701, Korea

Introduction

The outermost layer of the epidermal cell wall plays multiple roles (Carver and Gurr 2006; Leveau 2006; Pfündel et al. 2006), including the prevention of water loss from the cell surface and defense against pathogens or insects. This layer also protects plants from UV irradiation damage and prevents fusions between organs during plant development. It typically comprises the crystal epicuticular waxes deposited on the cuticle proper as well as a cuticular layer encrusted with intracuticular waxes in transit to polysaccharides (Kunst and Samuels 2003; Shepherd and Wynne Griffiths 2006).

Wax crystals are present in various shapes: tubule, fine rod, star-like rod, globule, and circular platelet (Baker 1982; Gulz 1994; Jetter and Riederer 1994; Beattie and Marcell 2002; Ao 2006). Although tubules and platelets are abundant, in rice the platelet and star-like rod types appear most frequently (Avato 1987; Yu et al. 2008). Species-unique cuticular wax components are postulated to organize themselves into crystallines and amorphous zones of the cuticle (Kirsch et al. 1997). When the concentration of a certain component reaches a critical threshold,

epicuticular crystalloids can arise, on the aerial surface, from the amorphous wax mixture that is embedded in the cutin polymer (Jetter and Riederer 1994; Jeffree 1996).

Most wax mutants, such as *eceriferum1* (*cer1*), *cer2*, *cer3*, *cer4*, *cer5*, *cer6*, *glossy1* (*gl1*), *gl8*, and *wax deficient anther1* (*wda1*), have less crystal wax on their cell surfaces (Lemieux 1996; Hansen et al. 1997; Xu et al. 1997; Jung et al. 2006). However, some show an altered epicuticular wax structure. For example, *knb1* mutants contain smaller flake-like wax crystals and *bcf1* mutants possess smaller plate-like crystals as well as long, slender, ribbon-like crystals (Jenks et al. 1996). In *gl1* and *gl26* mutants, their crystal shapes are changed from platelet-type to globule-type (Beattie and Marcell 2002). *gl1* also manifests a pleotropic effect, e.g., less wax, small trichomes, and a thin cuticle membrane structure. GL1 is a membrane-bounded desaturase/hydroxylase (Sturaro et al. 2005).

Cutin is composed of inter-esterified hydroxyl and hydroxyl epoxy fatty acids derived from common cellular fatty acids, mostly C16–C18 fatty acids with ω- and mid-chain hydroxyl groups (Kolattukudy 2001). However, α, ω-dicarboxylic fatty acids are the major cutin monomers in *Arabidopsis*, where ω-hydroxy and mid-chain hydroxylated fatty acids are also found (Bonaventure et al. 2004; Franke et al. 2005). Although the predominant cutin monomers are known, some unidentified components in cutin polymer and structure are poorly understood. In addition, mutants with a defective cutin matrix and/or inadequate organization are rare. Although the synthesis of cutin must be coordinated with extension of the cell surface during growth, how this is achieved also remains unsolved.

A defect in *LACERATA* (*LCR*) encoding a cytochrome P450 of the CYP86 family is implicated in the epidermal biosynthesis of cutin, causing cutin deformation and organ fusion (Wellesen et al. 2001). *Aberrant induction of type three genes 1* (*ATT1*) encodes a cytochrome P450 monooxygenase, catalyzing fatty acid oxidation for the biosynthesis of extra-cuticular lipids. In *att1*, cutin content is reduced to 30% and the cuticle is loosely organized, thereby increasing the transpiration rate two-fold (Xiao et al. 2004). The *eibi1* mutant is essential for drought resistance in barley. Normally, *EIBI1* functions in the cuticle as the transport-limiting layer; *eibi1* has the highest relative rate of water loss among the known wilt mutants. Leaves of *eibi1* have high stomatal density and a great chlorophyll efflux in 80% ethanol (Chen et al. 2004). *Sorghum bicolor bloomless22* (*bm22*) mutants also show a reduced cuticle thickness and increased water loss (Jenks et al. 1994). In contrast, the amount of cutin is enhanced in the *bodyguard* (*bdg*) mutant even though the cuticle is loosely organized (Kurdyukov et al. 2006). There, mutant plants exhibit strong growth retardation and abnormal leaf morphology. When immersed in 80% ethanol, leaves of *bdg* release chlorophyll faster than do wild-type leaves.

Here, we describe the identification of a rice mutant defective in its organization of cuticle and wax crystals, which leads to increased water loss via diffusion from the leaf surface.

Materials and methods

Plant materials and growing conditions

Generation of T-DNA tagging rice plants (*Oryza sativa* ssp. *japonica* cv. Dongjin and Hwayoung) has been reported previously (Jeon et al. 2000; Jeong et al. 2002). Seeds were germinated on a 1/2 MSO medium solidified with 0.2% phytagel and 0.55 mM *myo*-inositol (Sigma–Aldrich) in a closed container. The seedlings were grown for 1 or 2 weeks at 30°C under continuous light. They were then transplanted to soil in the greenhouse or paddy field for an additional 2 weeks of development.

Isolation of *wdl1* knockout plants

Three *wdl1* knockout alleles were isolated from the rice-flanking sequence database (http:://www.postech.ac.kr/life/pfg) (An et al. 2005a, b). T2 progeny of the primary insertional mutants were grown to maturity for seed amplification. Genotypes of *wdl1-1* were determined by PCR with the following primers: F1 (5′-ACCAGATCAA GTGGAGTGGA-3′), R1 (5′-AAAGGCAACAGTCAAGC AAG-3′), and LB-1 (5′-CATCTTGAAC GATAGCCTT T-3′). For genotyping *wdl1-2*, primers F2 (5′-CTCGCAT CTTGATTCCTCAT-3′), R1, and LB-1 were used; for *wdl1-3*, F3 (5′-CGTGCAACCTTCTTTGGTAA-3′), R2 (5′-CCATTGGATAGTCCTGTGGA-3′), and RB-1 (5′-AT CCAGACTGAATGCCCACAGGC-3′).

Quantitative real-time PCR

Expression patterns for *WDL1* were measured by real-time PCR with a Roche LightCycler II. *UBQ* mRNA expression was used to normalize the expression ratio for a gene. Primers included 5′-GATGGACCTGAAGGTGGTT-3′ and 5′-AACCACCTTCAGGTCCATC-3′ for *WDL1*, 5′-GGT GCTCAACACATCCACT-3′ and 5′-ATGCATTCTCTG CTCTCCT-3′ for *ABA2*, and 5′-CACGGTTCAACAA CATCCAG-3′ and 5′-TGAAGACCCTGACTGGGAAG-3′ for *UBQ*. Changes in gene expression were calculated via the $\Delta\Delta_{Ct}$ method.

Analyses by scanning electron microscopy and transmission electron microscopy

The second leaves from 7-day-old seedlings grown in a closed container were used for live SEM, and for SEM and TEM analyses. For live SEM, fresh samples were sputter-coated directly with palladium and examined with a scanning electron microscope (LEO 1450VP; Carl Zeiss, Jena, Germany). Other samples for SEM and TEM were pre-fixed for 3 h with 3% glutaraldehyde–sodium phosphate buffer (0.1 M) at room temperature and rinsed three times with 0.1 M sodium phosphate buffer. Post-fixation was performed with 2% OsO_4 at 4°C. The samples were dehydrated through an ethanol series and infiltrated with an isoamyl acetate series. TEM samples were sectioned 40–60 nm thick and then stained with 2.5% uranyl acetate before examination with a transmission electron microscope (JEOL 100CX-I, 80 kV; JEOL, Japan).

Analysis of leaf waxes and cutin

Before extracting wax, we scanned the leaves to calculate their surface areas. For total extraction, leaf blades and sheaths were excised from seedlings at 14 days after germination (DAG) and immersed for 1 h in 20 ml of $CHCl_3$ at 55°C (Haas et al. 2001). To avoid removing membrane lipids, the severing points of leaves were not immersed. As an internal standard, 20 μg of n-tetracosane (Fluka) was added to each sample. Chloroform was evaporated under a gentle stream of N_2 to a final volume of 100 μl. The wax samples were derivatized with 20 μl of pyridine and 20 μl of BSTFA (Machery-Nagel, Düren, Germany), then analyzed by GC–MS as previously described (Jung et al. 2006; Yu et al. 2008). Quantitative determination of wax components was based on the equivalent ratio of mass to peak area between the component and internal standard. Wax monomers were identified by mass spectrometry (Agilent Technologies, Böblingen, Germany). After this extraction, the same leaves were used in cutin analysis performed as described by Franke et al. (2005).

Determination of transpiration and conductance

Transpiration rates were measured with a steady-state porometer (LI-1600; LI-COR Bioscience, Lincoln, NE, USA) using 50 DAG plants grown under greenhouse conditions (Koizumi et al. 2007; Woo et al. 2007). The clip of a porometer evaluated water movement for each sampled leaf for 1 s and then recorded the value. Day and night evaporation rates were measured at 2 p.m. and 11 p.m.

Cell numbers and leaf fresh weights

Aerial parts from plants grown for 7 days in a closed container were held at 30°C and 40% relative humidity. For each genotype, the fresh weights of excised leaves were measured for water loss at 0, 5, 10, 20, 30, 60, 120, and 180 min. To count the number of stomatal and pavement cells per unit area, we attached the second leaves from 7 DAG seedlings to adhesive tape. Their epidermal and mesophyll cells were then removed through washing, leaving an epidermal cell trace on that tape. Densities of the stomatal and epidermal pavement cells, as well as the stomatal index of adaxial surfaces, were determined according to the procedure of Gray et al. (2000).

Chlorophyll leaching assay

After 7-day-old seedlings were air-dried for 6 h, leaf samples were incubated for 1 h in 80% ethanol at 37°C. The amount of extracted chlorophyll was measured at A647 and A664 nm on a UV-1,700 Pharmaspec spectrophotometer (Shimadzu). Chlorophyll concentrations were calculated as described previously (Lolle et al. 1997).

Vector construction and sub-cellular localization

The coding region of *WDL1* cDNA was PCR-amplified with primers 5′- CCCGGGATGCTTGGTTTTGCGCCG-3′ (the ATG start codon of Os*WDL*1 is underlined) and 5′-ACTAGTGTCCCATTGGATAGTCCTGT-3′ (the TAG stop codon was deleted to make a reading-frame fusion between *WDL1* and *sGFP*). The fragment was cloned into the *Sma*I and *Spe*I sites between the maize *Ubiquitin* promoter and the *sGFP* coding sequence (Moon et al. 2008). A vector containing the *AtBIP–mRFP* fusion was obtained from Inhwan Hwang (Park et al. 2004). Protoplasts were produced from rice mesophyll cells as follows. Leaves of 7 DAG seedlings were diced with a razor blade and incubated in a cell wall digestion-enzyme solution containing 1.5% cellulase, 0.3% macerozyme, 0.1% pectolyase, 0.6 M mannitol, 10 mM MES, 1 mM $CaCl_2$, and 0.1% (w/v) bovine serum albumin for 4 h at 26°C with gentle agitation (75 rpm), as described previously (Moon et al. 2008). Protoplasts (1×10^6 per ml) were mixed with 10 μg each of *WDL1-sGFP* and *AtBIP-mRFP* DNAs, then electroporated in 4-mm-wide cuvettes with a Gene Pulser Xcell (BioRAD, Baltimore, MD, USA) that was set at 300 V and 450 μF. For transient expression in onion cells, the epidermis was bombarded via the biolistic particle delivery system (PDS−1,000, Dupont), with parameters of 0.4 mg per shot of gold beads coated with about 2 μg per shot of each plasmid DNA and 900 psi of pressure in a 25-in. Hg

vacuum. After 10 to 15 h of incubation at 25°C under darkness, the transformed protoplasts and onion epidermal cells were examined on a Zeiss Axioplan fluorescence microscope equipped with filter sets for GFP and RFP.

Results

Isolation of the *wdl1* mutant from T-DNA tagged lines

We isolated a conditional lethal mutant line, 3A-07662 (cv. Dongjin), from a T-DNA insertional mutant population in japonica rice (Jeon et al. 2000; An et al. 2003; Lee et al. 2003; Ryu et al. 2004). These mutant plants were recessive-lethal in the paddy field. Mutant seeds produced from heterozygous plants germinated normally, but the seedlings showed a severe growth retardation phenotype and died within 30 days. However, when cultured under high humidity (more than 90% relative humidity), plants grew for an extended period although their stems and leaves were shorter than normal (Fig. 1a, b). Under low humidity, i.e., 40%, leaves of those mutants wilted within 10 min (Fig. 1c, d). Most mutant plants grown under normal greenhouse conditions died (Fig. 1e) but some occasionally survived to maturity and produced sterile spikelets (Fig. 1f). These survivors were shorter and their leaves fragile compared with their segregating wild-type siblings (Fig. 1f). Such phenotypes appeared to arise from sensitivity to dehydration. We named this mutant *wilted dwarf and lethal 1* (*wdl1*).

T-DNA insertional mutations in *WLD1*

Sequence analysis of the T-DNA flanking region from the mutant revealed that T-DNA was inserted into LOC_Os11g48070 (http://tigrblast.tigr.org/euk-blast/) on Chromosome 11. Its full-length cDNA was identified as AK067429 in the Knowledge-based Oryza Molecular Biological Encyclopedia (KOME) (http://cdna01.dna.affrc.go.jp/cDNA). The primary structure of *WDL1* comprises six exons and five introns (Fig. 2a). In *wdl1-1*, T-DNA is located 1,203 bp downstream from the ATG start codon, in the second intron of the gene.

The predicted protein encoded by *WDL1* contains 260 amino acid residues, with a molecular mass of approximately 28 kDa. This protein is 63% identical to cowpea CPRD49 (CowPea clones Responsive to Dehydration 49, BAB33036.1), which is induced by dehydration (Iuchi et al. 1996). WDL1 is also 67% identical to At3g11210 (AAM63310.1) and 51% to At2g38180 (AAL31218.1). Functional-domain analysis with Pfam 7.0 (http://www.sanger.ac.uk/Software/Pfam) indicated that the region between the 13th and 207th amino acid residues is highly conserved among these proteins (Fig. 2b). This region contains the conserved motifs found in SGNH subfamily proteins, which are members of the GDSL lipase superfamily (Akoh et al. 2004). SGNH proteins have four invariant catalytic residues—Ser, Gly, Asp, and His—in blocks I, II, III, and V, respectively (Fig. 2b; Akoh et al. 2004). WDL1 contains these conserved residues at Ser19, Gly48, Asp83, and His194. Phylogenic analysis using the MEGA 2.0 program indicated that the WDL1 protein is distantly related to other members of the GDSL lipase gene family (Fig. S1). From the flanking sequence database of T-DNA insertion sites (An et al. 2003; Jeong et al. 2006), we identified two additional alleles: *wdl1-2* (in the first intron) and *wdl1-3* (in the fifth exon) from Lines 4A-01860 (cv. Dongjin) and 1B-07129 (cv. Hwayoung), respectively (Fig. 2a). Quantitative RT PCR analyses of RNA extracted from homozygous mutant plants indicated that those three were null alleles (Fig. 2c). All had the same wilted dwarf phenotype and most died as seedlings. Therefore, we concluded that these phenotypes are due to the disruption of *WDL1* expression.

Because our insertional lines showed conditional mutant phenotypes, we examined whether gene expression is inducible. Although not influenced by all types of stress, transcript levels were reduced by wounding, drought, salt, and ABA treatments (Lee et al. 2006; Fig. 3a). As a control we also measured *ABA2* transcript levels during these trials (Rabbani et al. 2003); as expected, those were increased by such treatments (Fig. 3b), indicating that our stresses were properly applied. Although *WDL1* was expressed in whole plants, transcript levels were higher in the shoots and young panicles than in the calli and roots (Fig. 3c). Levels were also high in the reproductive organs.

wdl1 mutations affect epidermal permeability

Because *wdl1* mutants wilted under low humidity, we examined the surface structure of their leaf blades and found that the stomatal and pavement cells were smaller than in the wild type (WT) (Fig. 4a–d). This decrease in size was also associated with a higher number of stomatal and pavement cells per unit area. The ratio between the two cell types was increased by about 12% in the mutant (Fig. 4e).

The transpiration rates for mutant plants were 2.3 times higher during the day compared with their WT siblings (Fig. 5a, b). Chlorophyll leaching assays are used for measuring the non-stomatal permeability that is presumably indicative of water loss (Yoshida et al. 2002). To minimize the water loss through the stomata during our assay, we dried the leaf samples for 6 h before treating with 80% ethanol. It was previously reported that detached leaves close their stomata within 30 min (Kerstiens et al. 2006). Chlorophylls were extracted three- to four-fold

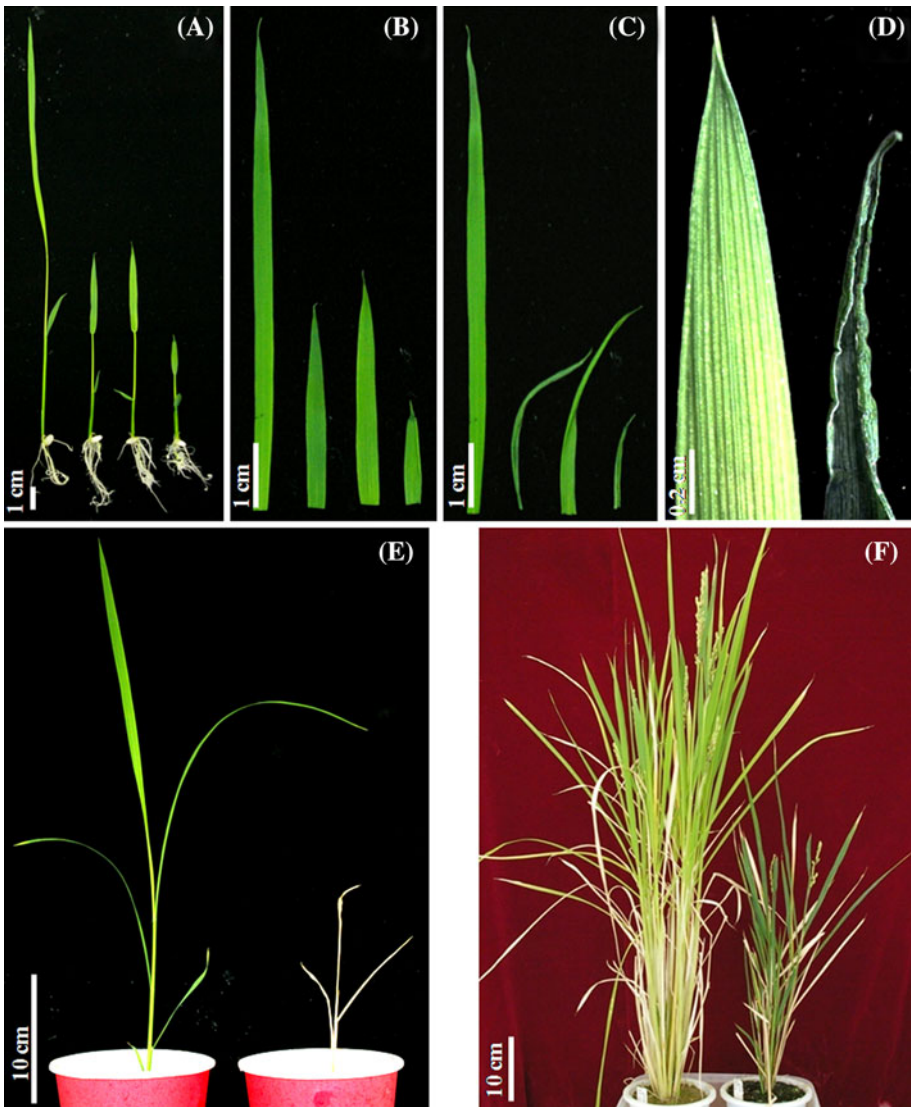

Fig. 1 Phenotypes of rice seedlings. **a** Heights of WT (*left*), *wdl1-1* (2nd from *left*), *wdl1-2* (3rd from *left*), and *wdl1-3* (*right*) grown in closed container for 7 days after germination (DAG). **b** Third leaves of 7 DAG plants in same order as **a**. **c** Detached leaves were dried for 20 min at room temperature. **d** Enlargement of **c** at tip region. **e** Plants grown for 7 additional days in soil under natural conditions. *Left*, WT; *right*, *wdl1-1*. **f** WT (*left*) and *wdl1-1* (*right*) plants at mature stage

more rapidly from all three *wdl1* seedlings relative to the WT (Fig. 5c, d). All mutants lost water more quickly over the first 30 min (Fig. 5e). These data indicated that conductance is faster in *wdl1*, probably due to non-stomatal diffusion through their leaf surfaces.

The cuticle is abnormal in *wdl1* mutants

SEM analyses showed that the WT leaf surface was covered evenly with hairy crystal waxes (Fig. 6a–c). This is consistent with previous reports (Sánchez et al. 2003; Jung et al. 2006; Yu et al. 2008). In contrast, the leaf surfaces of *wdl1* mutants grown under the same conditions of high humidity were covered by both normal and disorganized crystal waxes, including a split wax cluster, curdled wax, and a stretched wax curd (Fig. 6e–g, i–k). To confirm that these changes were not due to any alteration during sample preparation we examined the surfaces with a live SEM. Our analyses presented the same results, i.e., abnormal waxes on the mutant surface (Fig. 6c, g).To examine whether the substances from those mutant and WT leaves are indeed waxes, we washed the samples with 100% chloroform (Haas et al. 2001). Images obtained after this washing demonstrated that the surfaces were cleaned in both types (Fig. 6d, h). These results demonstrated that mutations in *WDL1* affect wax crystallization and distribution on the leaf surface. Cross-sectioning of the WT showed that the cuticle was even, flat, and regular (Fig. 7a, f) whereas the *wdl1* cuticle was loosely packed and had unclear boundaries, uneven thickness, and less compactness (Fig. 7b–e, g–j). Cell walls of the WT were of even and regular thickness (Fig. 7a) compared with an irregular and fluctuating thickness from the mutant (Fig. 7b–e).

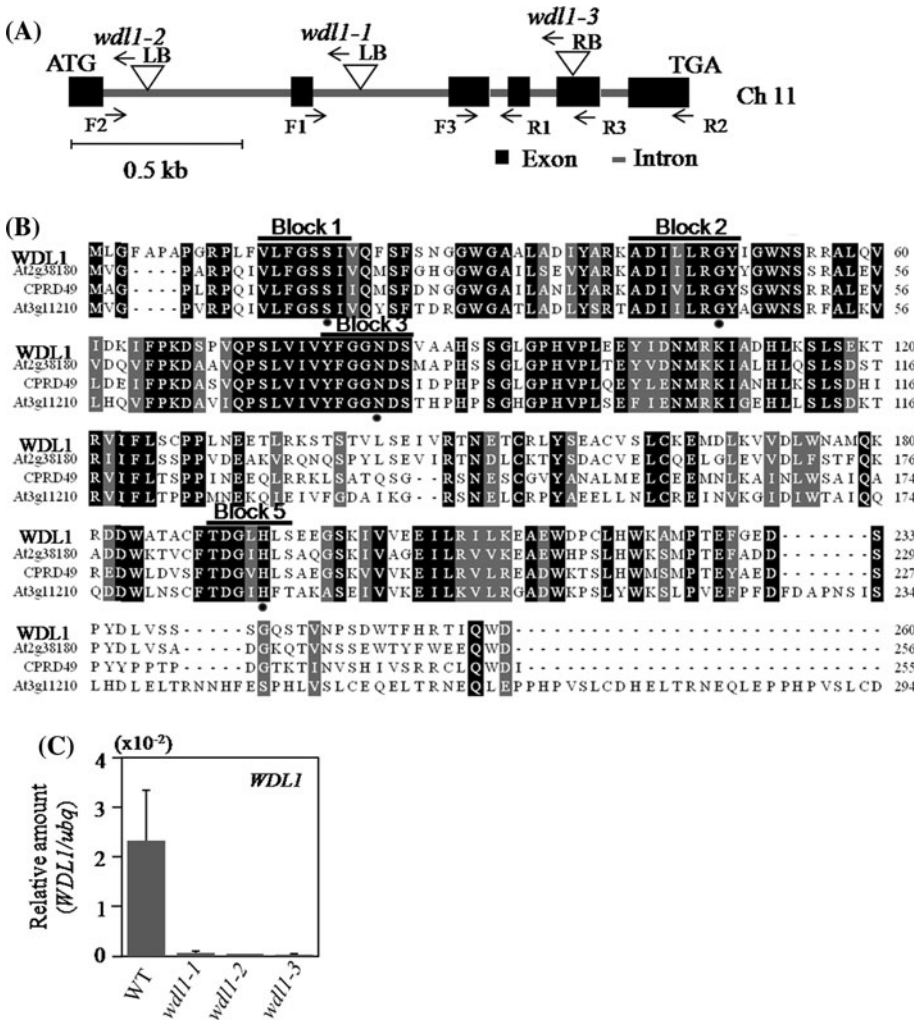

Fig. 2 Isolation of *wdl1* knockout plants. **a** Schematic diagram of *WDL1* and insertion positions of T-DNA. *Closed boxes* represent 6 exons; connecting *black lines* are 5 introns. *Horizontal arrows* indicate primers used for genotyping T2 progeny. **b** Alignment of amino acid sequences of SGNH proteins. *Black boxes* represent identical amino acids; *gray boxes*, similar amino acids. *Block*s are conserved domains; dots are active amino acids in SGNH subfamily. **c** Expression analysis of *WDL1* in WT and three *wdl1* alleles by quantitative real-time PCR. *Y* axis, relative values between transcript levels of *WDL1* and *UBQ*; *vertical bars*, standard deviation

WDL1 protein localizes in the ER

Because the *wdl1* cuticle was abnormal, we hypothesized that the WDL1 protein is involved in wax and cutin formation. If true, that protein would likely be localized to the endoplasmic reticulum, where most wax and cutin biosynthesis occurs. Therefore, we made a fusion of the synthetic GREEN FLUORESCENCE PROTEIN (sGFP) at the C-terminal of WDL1 (Fig. 8a, upper). As a positive control, we used the previously characterized AtBIP–mRFP that is localized to the ER (Fig. 8a, lower; Park et al. 2004). When these chimeric molecules were co-introduced into rice mesophyll protoplasts prepared from 10-day-old seedlings, the GFP signal from WDL1–GFP coincided with the RFP signal driven by the AtBIP–mRFP protein (Fig. 8b–e). As a negative control, we used sGFP localized to the nucleus and cytoplasm (Fig. 8f–h). Similar results were obtained when these fusion molecules were introduced into onion epidermal cells (Fig. 8i–k), thereby indicating that WDL1 is an ER protein and may be related to wax and cutin biogenesis.

Amounts of wax and cutin are not significantly changed in *wdl1*

Leaves of *wdl1* had a disorganized epicuticular crystal wax layer and deformed epidermal cell arrangement. To determine whether this abnormality is due to a change in wax composition in the cuticle, we sampled leaves from WT and *wdl1* plants grown for 14 days under high humidity. Epicuticular waxes were extracted with chloroform and analyzed by GC–MS. The total amounts of wax did not differ significantly (Fig. 9a), and detailed analyses showed that the amounts of fatty acids, aldehydes, alkanes, and esters also remained the same. However, the content of primary alcohol monomers was slightly increased in the mutant (Fig. 9b), a change mainly due to a rise in C30 alcohol (Fig. 9c).

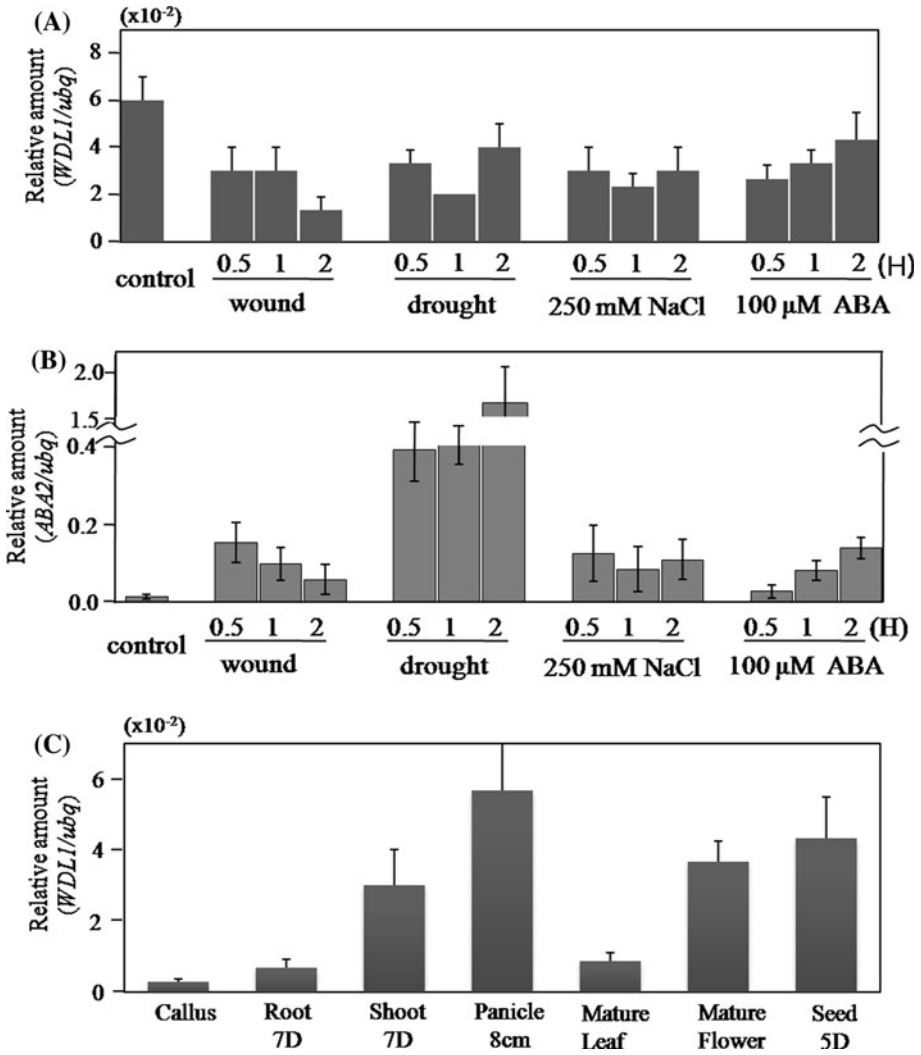

Fig. 3 *WDL1* gene expression pattern. **a** *WDL1* transcript levels after treatment by wounding, drought, 250 mM NaCl, or 100 µM ABA for 30 min, 1 h, or 2 h. **b** *ABA2* expression after same treatments as **a** for 30 min, 1 h, or 2 h. **c** *WDL1* expression patterns in callus, root at 7 DAG, shoot at 7 DAG, panicle <8 cm, mature leaf at 80 DAG, mature flower, and seed at 5 days after pollination. *Y* axis, relative *WDL1* transcript level; *vertical bar*, standard deviation

We also analyzed cutin that remained after the epicuticular wax was extracted. This represented the lipid polymers, e.g., cutin and other covalently bound lipids, attached to the cell wall (Franke et al. 2005; Kurdyukov et al. 2006). Here, the mutants and wild type did not differ significantly in their amounts of cutin (Fig. 9d, e).

Discussion

Wilt phenotype is associated with increased permeability

We have now identified T-DNA insertional mutants that are dwarf and lethal when grown under normal humidity. There phenotypes are associated with a higher day time transpiration rate. Our chlorophyll leaching assay suggested increased permeability of the *wdl1* leaf surface. Although the contribution of stomatal and non-stomatal water loss during the day has not yet been determined, our results suggest that *wdl1* mutants might lose water more rapidly, at least partially because of enhanced cuticle-membrane permeability. TEM examination showed that the cuticle of *wdl1* is loose and irregular, which likely accounts for this greater permeability. The *wdl1* cuticle membrane is also thicker and uneven, with such morphological changes probably leading to enhanced conductance.

Although some researchers have reported no clear relationship between cuticle water permeability and physical properties, e.g., thickness, coverage, and uniformity (Riederer and Schreiber 2001; Kerstiens 2006), analysis of *Sorghum bicolor bloomless* (*bm*) mutants with an altered epicuticular wax structure has identified a mutation affecting the deposition of both epicuticular wax and cuticle (Jenks et al. 1994). The cuticle from *bm* plants is about 60% thinner and only 20% of the WT weight. This diminished cuticle deposition is correlated with increased epidermal conductance. Similar observations have been made with the

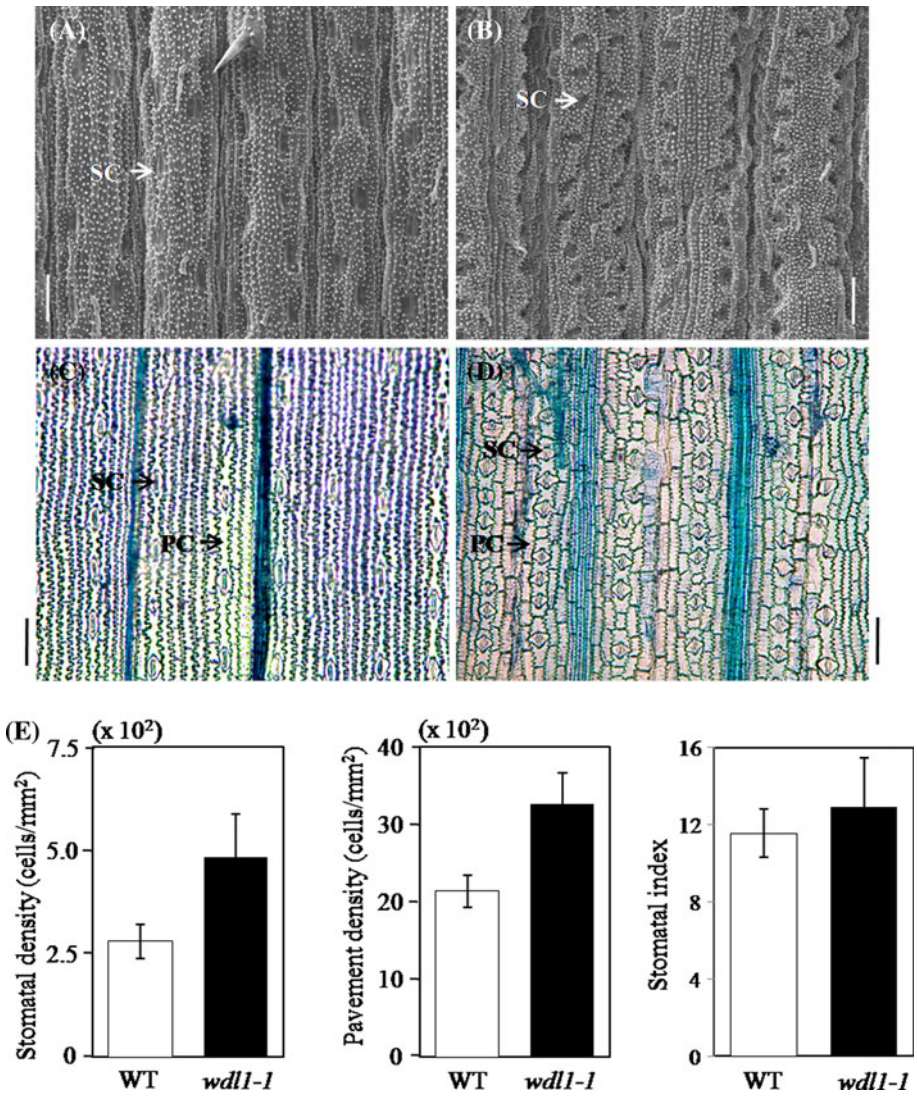

Fig. 4 Analyses of stomatal cell (*SC*) and pavement cell (*PC*) densities. **a**, **b** SEM and **c**, **d** optical microscopy of cells in adaxial region of 2nd leaves from **a**, **c** WT and **b**, **d** *wdl1-1* plants. *Scale bars* are 50 μm. **e** SC density, PC density, and stomatal index in adaxial region of 2nd leaves. For each genotype, 24 samples were measured from 5 leaves. Stomatal index is number of stomata as percentage of total cells

Arabidopsis wax2 mutant, in which the cuticle is thicker and structurally disorganized (Chen et al. 2003). *Lacs2* (*Long-Chain Acyl–CoA Synthetase 2*) has a thinner abaxial cutin and an increased rate of chlorophyll leaching (Schnurr et al. 2004). The *att1* mutant, in which cutin content is reduced to 30%, also has a loose cuticle and greater permeability to water vapor (Xiao et al. 2004).

Because our mutants also presented a loosely packed and uneven cuticle, we should have expected a change in the cutin amount but, instead, found no significant alteration in total cutin and cutin monomer levels. Therefore, *WDL1* does not appear to be involved in cutin monomer biosynthesis, making it probable that the gene product affects cutin polymer organization. Nevertheless, it is still unknown what determines this organization. In *att1* and *bm* mutants, the cuticles are loose due to a lower cutin content that results in more rapid transpiration (Xiao et al. 2004). This would suggest that reducing cutin levels affects the structure of the cuticle. However, a higher level of cutin in *bdg* mutants also causes the cuticle proper to be less dense, implying that compactness is not always correlated with cutin amount (Kurdyukov et al. 2006). Therefore, other factors must control this organization. Because our *wdl1* mutants have an altered structure in their cuticle membrane but little change in the level of cutin, we might conclude that the *WDL1* gene product is involved in cutin organization. This finding is similar to that reported for the *wax2* mutant, where no effect is found on cutin amount even though plants have a thicker and less opaque cuticle proper (Rowland et al. 2007). Cutan, a non-depolymerizable or unsaponifiable polymethylene biopolymer that is associated with the cuticle membrane (Schreiber 2005), plays an important role as a barrier to the sorption of polar and non-polar substances, as well as other aromatic compounds

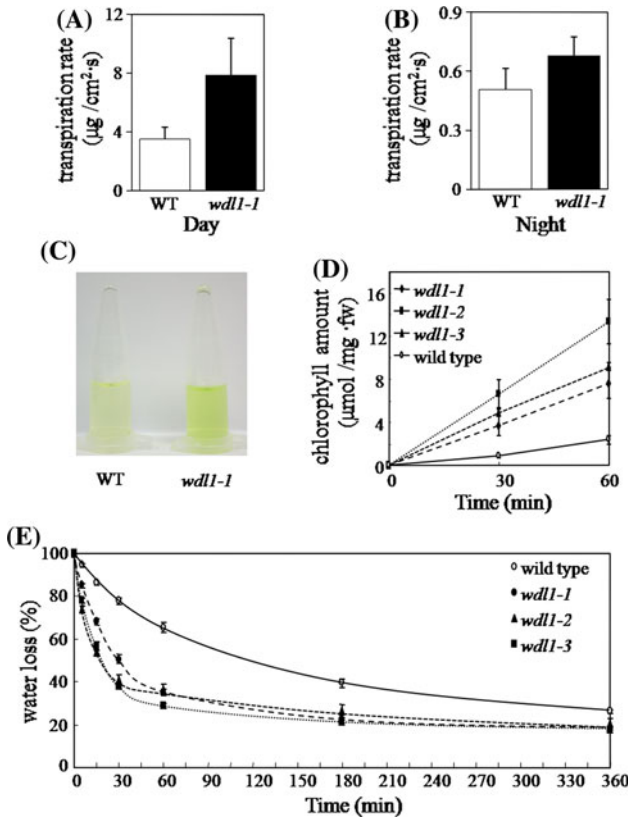

Fig. 5 Physiological characterization of *wdl1* mutants. Water evaporation rates were measured at 2 p.m. (**a**) and 11 p.m. (**b**). **c** Chlorophyll extraction for 60 min. **d** Chlorophyll leaching from WT and mutants. **e** Percentage of fresh weight reduction in detached leaves under 40% relative humidity at 30°C. Experiments were repeated 3 times. *Each bar* indicates mean ± SD from 3 replicates

(Stimler et al. 2006). Because we did not compare the amount, composition, and organization or arrangement of cutan between mutant and wild type, we cannot exclude the possibility that different cutan levels can account for the differences in transpirational and chlorophyll leaching rates in the *wdl1* mutant. Alternatively, WDL1 could indirectly affect the cuticle. For example, although *SHN* gene is not involved in cutin biosynthesis, overexpression of the gene exerted influence in deforming cuticle structure and increased cuticle permeability (Aharoni et al. 2004). The gene is a member of AP2/EREBP transcription factors that activates terpenoid biosynthesis.

Abnormal wax crystals are likely due to an irregular cuticle

Because *wdl1* mutants have an altered epicuticular wax structure, we predicted a significant change in the amount and composition of wax compared with the WT. However, the levels of fatty acids, aldehydes, alkanes, and esters remained constant, while only a slight increase was observed in the primary alcohols, especially the C30 chain length. Because these primary alcohols are the major component of waxes, it is possible that a rise in their levels modifies the overall organization of those waxes. For example, a 1.6-fold increase in alkanes and primary alcohols in *knb1* accompanies a change in the wax crystal structure (Jenks et al. 1996) while a decline in wax monomer levels also affects the epicuticular wax structure. In *cer4* mutants, the levels of C24, C26, C28, and C30 primary alcohols are severely reduced, and the wax crystal structure shifts to a vertically oriented plate-like shape (Rowland et al. 2006).

When the amount of wax exceeds a critical threshold, crystals are generated from the wax mixture that is embedded in the crosslinked cutin (Jetter and Riederer 1994; Jeffree 1996; Kirsch et al. 1997). Because of the loose, uneven, and variable arrangement in the cuticle membrane and cell walls of our *wdl1* mutants, it is possible that wax is irregularly secreted, thereby leading to disorganized deposition.

Defects in the cuticle are not compensated for by a greater amount of epicuticular wax. For example, in *bdg* mutants with a 3.5-fold increase in wax content, chlorophyll is extracted twice as fast as from the wild type (Kurdyukov et al. 2006). Furthermore, although *shn* has six-fold more wax per unit area compared with the WT, its rates of chlorophyll and water extraction are eight-fold and six-fold faster, respectively (Aharoni et al. 2004).

WDL1 is likely involved in a later step of cutin formation

WDL1 is homologous to SGNH subfamily proteins, which are members of the GDSL lipase superfamily (Akoh et al. 2004). That superfamily comprises a diverse group of hydrolases, including lipases, esterases, thioesterases, arylesterases, proteases, and lysophospholipases. These enzymes display various functional properties, such as broad substrate specificity and region specificity (Akoh et al. 2004). Compared with common lipases, the GDSL lipases have a flexible active site that changes conformation in the presence of substrate. WDL1 has a catalytic triad consisting of the Ser19, Asp191, and His194 residues in the active center of the SGNH family proteins (Ling et al. 2006). A group of SGNH lipases has been characterized as sinapine esterase (Clauβ et al. 2008). In addition to sinapine esterase activity, the SGNH lipases show broad substrate specificity toward various choline esters, including phosphatidylcholine. To investigate whether WDL1 is a lipase, we examined acyl-hydrolase activity of heterologously expressed protein, using 4-nitrophenyl derivatives as substrates. Although we were unable to demonstrate

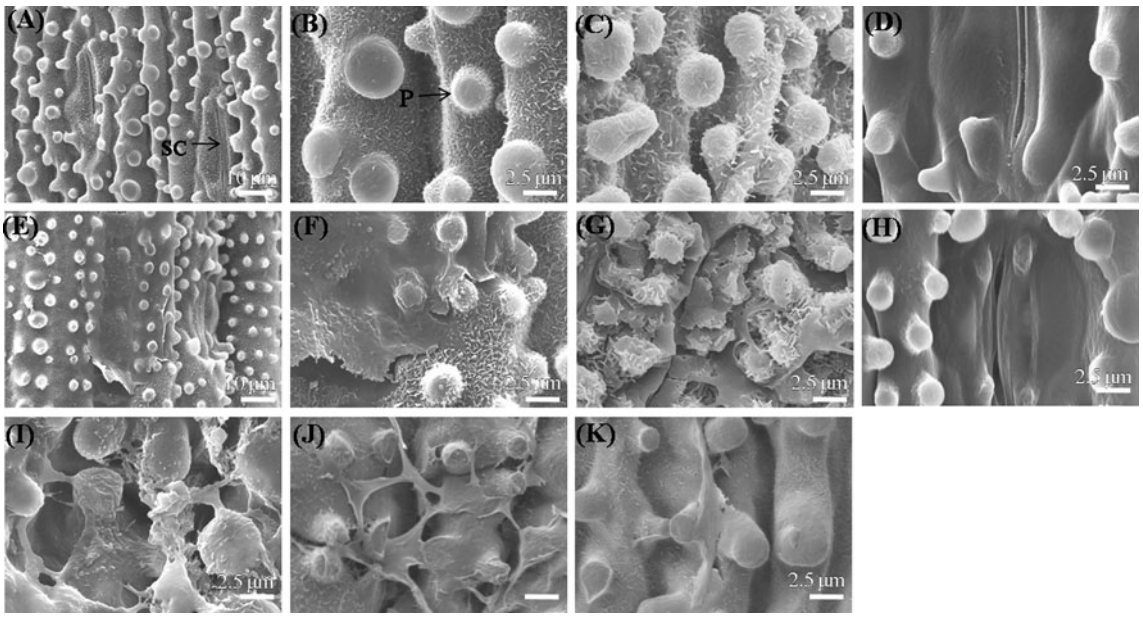

Fig. 6 Scanning electron microscopy analyses of adaxial leaf surfaces from WT, *wdl1-1*, *wdl1-2*, and *wdl1-3*. **a**–**c** WT showing star-type wax crystals. **e**–**g**,**i** SEM of *wdl1-1*. Live SEM for WT (**c**) and *wdl1-1*(**g**). SEM for WT (**d**) and *wdl1-1*(**h**) after wax was removed by chloroform. **j** *wdl1-2*, and **k** *wdl1-3*. **f** Star-type and split-wax cluster, **i** curdled wax structure, **j** stretched curd wax and. P, papillae; SC, stomata cell. *Scale bars* are 10 μm (**a**, **d**) and 2.5 μm (**c**, **e**–**k**)

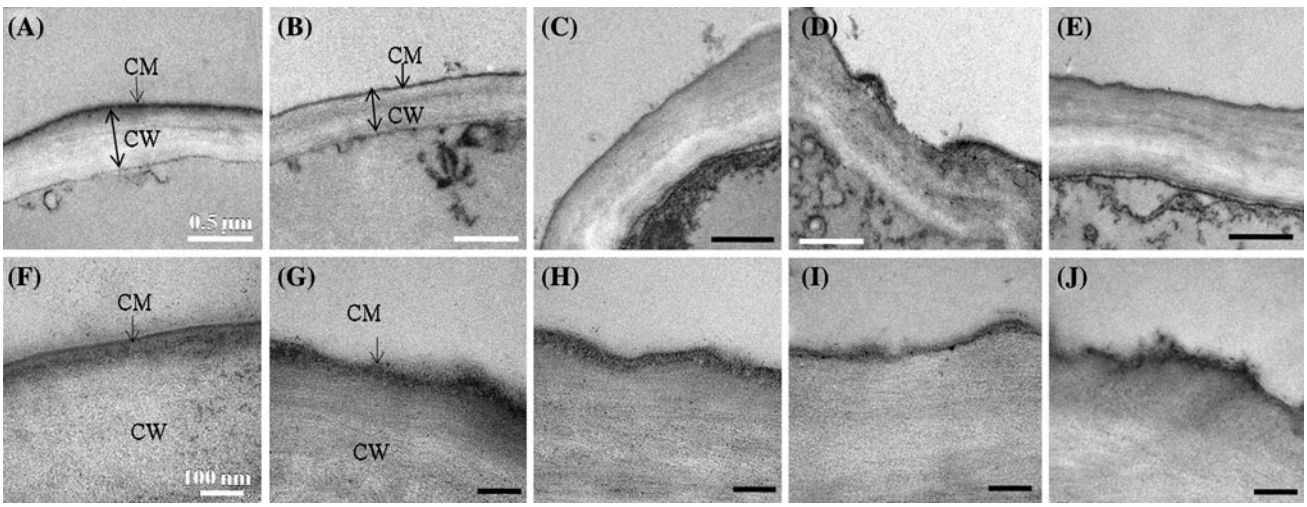

Fig. 7 Transmission electron microscopy analyses of adaxial leaf epidermis from 7-day-old seedlings. (**a**, **f**) WT showing even thickness, regular compactness, and clear cuticle boundary. (**b**–**e**, **g**–**h**) TEM of *wdl1-1* with uneven thickness, less compactness, and vague cuticle boundary (**g**), even but occasionally thin and irregular region (**h**). **i** TEM of *wdl1-2* and **j** *wdl1-3*. CM, cuticle membrane; CW, cell wall

hydrolase activity for WDL1 using this model substrate, the enzyme probably functions as a lipase because the protein shares high sequence homology with SGNH lipases and contains conserved residues in the active center of the SGNH proteins (Ling et al. 2006). However, either their very narrow substrate specificity hampers functional analysis or else this enzyme functions as part of a multi-complex system. We also cannot discount the possibility that WDL1 is active in the formation of ester linkages involving non-lipid cell wall components such as methylated and acetylated carbohydrates. Secondly, these could affect the anchorage of cutin polyester that disturbs the cuticular membrane.

WDL1 is co-localized with an ER marker protein, indicating that it is a protein within the endoplasmic reticulum. Because most wax and cutin monomers are

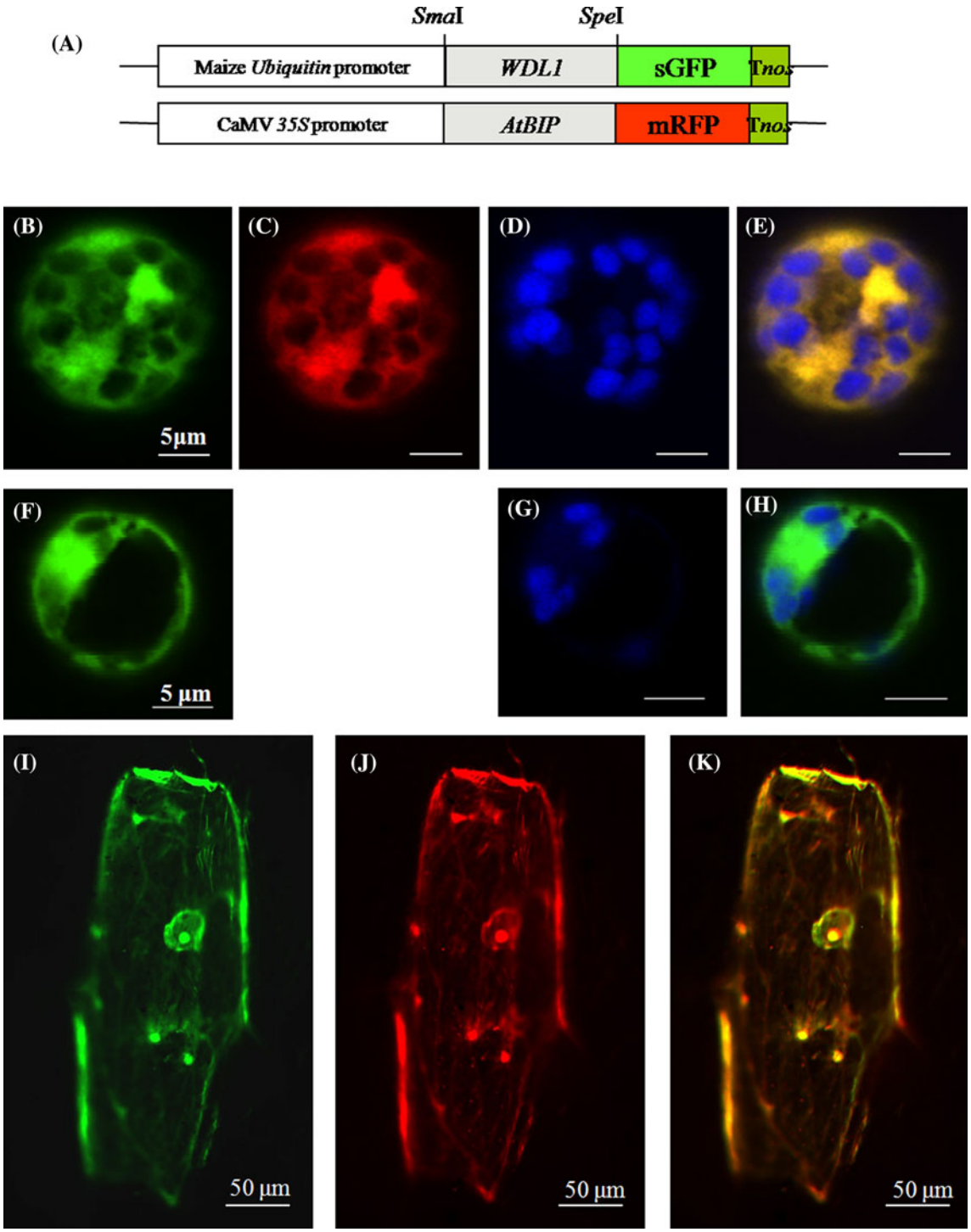

Fig. 8 Sub-cellular localization of WDL1–GFP. **a** Schematic diagrams of *35S:AtBIP–RFP* and *Ubi:WDL1–GFP*. (**b**–**e**) Sub-cellular localization of WDL1 in mesophyll cells. **b** Localization of WDL1–GFP protein and **c** AtBIP–RFP as ER marker. **d** Auto-fluorescence of chloroplast. **e** Merged image of **b**, **c**, and **d**. (**f**–**h**) Sub-cellular localization of sGFP in mesophyll cells. **f** sGFP image, **g** auto-fluorescence, and merged image of f and g **h**. (**i**-**k**) Sub-cellular localization of WDL1::GFP in onion epidermal cells. **i** WDL1–GFP, **j** AtBIP–RFP, and **k** merged images of **h** and **i**

synthesized there, results from our localization experiment demonstrate that WDL1 protein also plays a role either in providing or connecting and arranging the precursors for proper cuticle formation. Because our biochemical analyses did not reveal any significant alteration in the monomers, it is likely that WDL1 is involved in steps of cutin

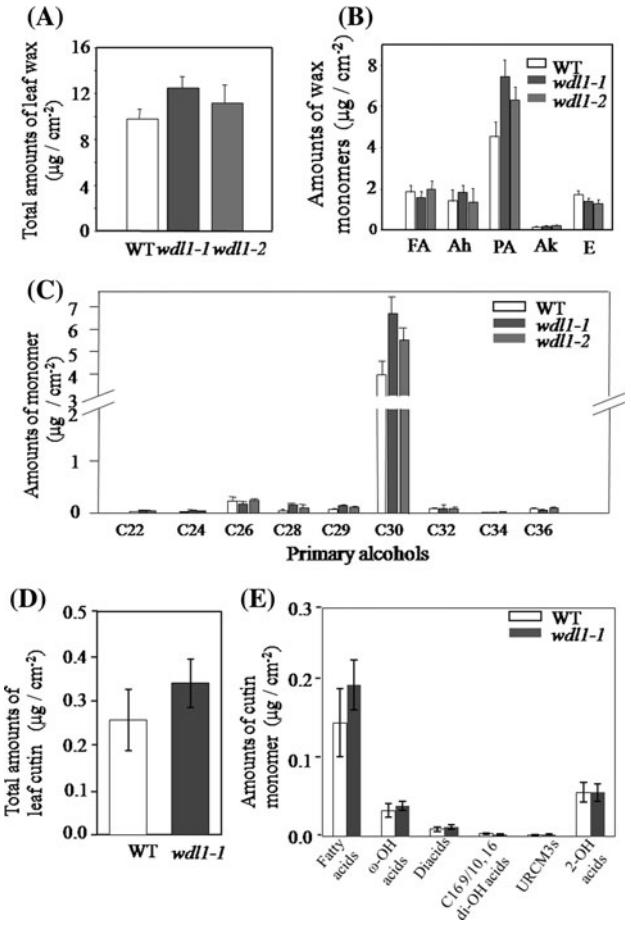

Fig. 9 Epicuticular wax and cutin comparative analyses. **a** Total wax in epicuticular region from WT, *wdl1-1*, and *wdl1-2*. Total waxes were prepared from 14 DAG seedlings grown under high humidity. **b** Wax monomers from WT, *wdl1-1*, and *wdl1-2*. Fatty acids (FA), Aldehydes (Ah), Primary Alcohol (PA), Alkanes (Ak), Esters (E). **c** Primary alcohols from WT, *wdl1-1*, and *wdl1-2*. **d** Total cutin amounts in cuticle layers from WT and *wdl1-1*. **e** Amounts of cutin monomers from WT and *wdl1-1*. *Each bar* indicates mean ± SD from 4 replicates; experiments were repeated 3 times

organization, perhaps by providing pre-formed oligomeric esters or inducing the modification of non-ester cross-links, e.g., C–C and C–O–C, of non-depolymerizable components.

Acknowledgements We thank Insoon Park and Kyungsook An for generating T-DNA insertional lines, Yoonja Cho for handling the seed stock, Yong Mok Park for providing the steady state porometer, Inhwan Hwang for the vector containing the *AtBIP*: *mRFP* fusion, and Priscilla Licht for English editing. This work was supported, in part, by grants from the Crop Functional Genomic Center, the 21st Century Frontier Program (Grant CG1111); from the Biogreen 21 Program (034-001-007-03-00), Rural Development Administration; and from the Basic Research Promotion Fund with a Korea Research Foundation Grant (KRF-2007-341-C00028); Technology Development Program for Agriculture and Forestry, Ministry for Food, Agriculture, Forestry and Fisheries, Republic of Korea (309,017-5); and Kyung Hee University to GA, and grants of the Deutsche Forschungsgemeinschaft (DFG) to LS and RF.

References

Aharoni A, Dixit S, Jetter R et al (2004) The SHINE clade of AP2 domain transcription factors activates wax biosynthesis, alters cuticle properties, and confers drought tolerance when overexpressed in *Arabidopsis*. Plant Cell 16:2463–2480

Akoh CC, Lee GC, Liaw YC et al (2004) GDSL family of serine esterases/lipases. Prog Lipid Res 43:534–552

An S, Park S, Jeong DH et al (2003) Generation and analysis of end sequence database for T-DNA tagging lines in rice. Plant Physiol 133:2040–2047

An G, Jeong DH, Jung KH, Lee S (2005a) Reverse genetic approaches for functional genomics of rice. Plant Mol Biol 59:111–123

An G, Lee S, Kim SH, Kim SR (2005b) Molecular genetics using T-DNA in rice. Plant Cell Physiol 46:14–22

Ao CQ (2006) Morphological characters of leaf epidermis in Schisandraceae and their systematic significance. J Plant Biol 49:80–87

Avato P (1987) Chemical genetics of epicuticular wax formation in maize. Plant Physiol Biochem 25:179–190

Baker EA (1982) Chemistry and morphology of plant epicuticular waxes. In: Cutler DF, Alvin KL, Price CE (eds) The plant cuticle. Academic Press, London, pp 139–165

Beattie GA, Marcell L (2002) Effect of alterations in cuticular wax biosynthesis on the physiochemical properties and topography of maize leaf surfaces. Plant Cell Environ 25:1–16

Bonaventure G, Beisson F, Ohlrogge J, Pollard M (2004) Analysis of the aliphatic monomer composition of polyesters associated with Arabidopsis epidermis: occurrence of octadeca-cis-6, cis-9-diene-1, 18-dioate as the major component. Plant J 40:920–930

Carver TLW, Gurr SJ (2006) Filamentous fungi on plant surfaces. In: Biology of the plant cuticle. pp 368–397

Chen X, Goodwin SM, Boroff VL et al (2003) Cloning and characterization of the *WAX2* gene of *Arabidopsis* involved in cuticle membrane and wax production. Plant Cell 15: 1170–1185

Chen G, Sagi M, Weining S et al (2004) Wild barley *eibi1* mutation identifies a gene essential for leaf water conservation. Planta 219:684–693

Clauβ K, Baumert A, Nimtz M et al (2008) Role of a GDSL lipase-like protein as sinapine esterase in Brassicaceae. Plant J 53: 802–813

Franke R, Briesen I, Wojciechowski T et al (2005) Apoplastic polyesters in *Arabidopsis* surface tissues–a typical suberin and a particular cutin. Phytochem 66:2643–2658

Gray JE, Holroyd GH, van der Lee FM et al (2000) The *HIC* signalling pathway links CO2 perception to stomatal development. Nature 408:713–716

Gulz PG (1994) Epicuticular leaf waxes in the evolution of the plant kingdom. Plant Physiol 143:453–464

Haas K, Brune T, Rücker E (2001) Epicuticular wax crystalloids in rice and sugar cane leaves are reinforced by polymeric aldehydes. J Appl Bot 75:178–187

Hansen JD, Pyee J, Xia Y et al (1997) The glossy1 locus of maize and an epidermis-specific cDNA from *Kleinia odora* define a class of receptor-like proteins required for the normal accumulation of cuticular waxes. Plant Physiol 113:1091–1100

Iuchi S, Yamaguchi-Shinozaki K, Urao T et al (1996) Novel drought-inducible genes in the highly drought-tolerant cowpea: cloning of cDNAs and analysis of the expression of the corresponding genes. Plant Cell Physiol 37:1073–1082

Jeffree CE (1996) Structure and ontogeny of plant cuticles. In: Kerstiens G (ed) Plant cuticles. BIOS Scientific Publishers, Oxford, pp 33–82

Jenks MA, Joly RJ, Peters PJ et al (1994) Chemically induced cuticle mutation affecting epidermal conductance to water vapor and disease susceptibility in *Sorghum bicolor* (L.) Moench. Plant Physiol 105:1239–1245

Jenks MA, Rashotte AM, Tuttle HA, Feldmann KA (1996) Mutants in *Arabidopsis thaliana* altered in epicuticular wax and leaf morphology. Plant Physiol 110:377–385

Jeon JS, Lee S, Jung KH et al (2000) T-DNA insertional mutagenesis for functional genomics in rice. Plant J 22:561–570

Jeong DH, An S, Kang HG et al (2002) T-DNA insertional mutagenesis for activation tagging in rice. Plant Physiol 130:1636–1644

Jeong DH, An S, Park S et al (2006) Generation of flanking sequence-tag database for activation-tagging lines in japonica rice. Plant J 45:123–132

Jetter R, Riederer RM (1994) Epicuticular crystals of nonacosan-10-ol: in vitro reconstitution and factors influencing crystal habits. Planta 195:257–270

Jung KH, Han MJ, Lee DY et al (2006) *Wax-deficient anther1* is involved in cuticle and wax production in rice anther walls and is required for pollen development. Plant Cell 18:3015–3032

Kerstiens G (2006) Water transport in plant cuticles: an update. J Exp Bot 57:2493–2499

Kerstiens G, Schreiber L, Lendzian KJ (2006) Quantification of cuticular permeability in genetically modified plants. J Exp Bot 57:2547–2552

Kirsch T, Kaffarnik F, Riederer M, Schreiber L (1997) Cuticular permeability of the three tree species *Prunus iaurocerasus* L., *Ginkgo biloba* L. and *Juglans regia* L: comparative investigation of the transport properties of intact leaves, isolated cuticles and reconstituted cuticular waxes. J Exp Bot 48:1035–1045

Koizumi K, Ookawa T, Satoh H, Hirasawa T (2007) A wilty mutant of rice has impaired hydraulic conductance. Plant Cell Physiol 48:1219–1228

Kolattukudy PE (2001) Polyesters in higher plants. In: Scheper T (ed) Advances in biochemical engineering/biotechnology, vol 71. Springer, Berlin, pp 1–49

Kunst L, Samuels AL (2003) Biosynthesis and secretion of plant cuticular wax. Progr Lipid Res 42:51–80

Kurdyukov S, Faust A, Nawrath C et al (2006) The epidermis-specific extracellular *BODYGUARD* controls cuticle development and morphogenesis in *Arabidopsis*. Plant Cell 18:321–339

Lee S, Kim J, Son JS, Nam J et al (2003) Systematic reverse genetic screening of T-DNA tagged genes in rice for functional genomic analyses: MADS-box genes as a test case. Plant Cell Physiol 44:1403–1411

Lee MO, Choi PG, Kim JA et al (2006) Two novel protein kinase genes, *OsMSRPK1* and *OsMSURPK2*, are regulated by diverse environmental stresses in rice. J Plant Biol 49:247–256

Lemieux B (1996) Molecular genetics of epicuticular waxes biosynthesis. Trends Plant Sci 1:312–318

Leveau JH (2006) Microbial communities in the phyllosphere. In: Riederer M, Müller C (eds) In: Annual plant reviews: biology of the plant cuticle 23. Blackwell, Oxford, pp 334–367

Ling H, Zhao J, Zuo K et al (2006) Isolation and expression analysis of a GDSL-like lipase gene from *Brassica napus* L. J Biochem Mol Biol 39:297–303

Lolle SJ, Berlyn GP, Engstrom EM et al (1997) Developmental regulation of cell interactions in the *Arabidopsis fiddlehead-1* mutant: a role for the epidermal cell wall and cuticle. Dev Biol 189:311–321

Moon S, Giglione C, Lee DY et al (2008) Rice peptide deformylase PDF1B is crucial for development of chloroplasts. Plant Cell Physiol 49:1536–1546

Park M, Kim SJ, Vitale A, Hwang I (2004) Identification of the protein storage vacuole and protein targeting to the vacuole in leaf cells of three plant species. Plant Physiol 134:625–639

Pfündel EE, Agati G, Cerovic ZG (2006) Optical properties of plant surfaces. In: Riederer M, Müller C (eds) Annual plant reviews 23: biology of the plant cuticle. Blackwell, Oxford, pp 216–249

Rabbani MA, Maruyama K, Abe H et al (2003) Monitoring expression profiles of rice genes under cold, drought, and high-salinity stresses and abscisic acid application using cDNA microarray and RNA gel-blot analyses. Plant Physiol 133: 1755–1767

Riederer M, Schreiber L (2001) Protecting against water loss: analysis of the barrier properties of plant cuticles. J Exp Bot 52: 2023–2032

Rowland O, Zheng H, Hepworth SR et al (2006) *CER4* encodes an alcohol-forming fatty acyl-coenzyme A reductase involved in cuticular wax production in Arabidopsis. Plant Physiol 142: 866–877

Rowland O, Lee R, Franke R et al (2007) The *CER3* wax biosynthetic gene from *Arabidopsis thaliana* is allelic to *WAX2/YRE/FLP1*. FEBS Lett 581:3538–3544

Ryu CH, You JH, Kang HG et al (2004) Generation of T-DNA gene tagging lines with a bidirectional gene trap vector and the establishment of an insertion-site database. Plant Mol Biol 54:489–502

Sánchez E, Montiel M, Espinoza AM (2003) Ultrastructural morphologic description of the wild rice species *Oryza latifolia* (Poaceae) in Costa Rica. Rev Biol Trop 51:345–353

Schnurr J, Shockey J, Browse J (2004) The acyl-CoA synthetase encoded by *LACS2* is essential for normal cuticle development in *Arabidopsis*. Plant Cell 16:629–642

Schreiber L (2005) Polar paths of diffusion across plant cuticles: new evidence for an old hypothesis. Ann Bot (Lond) 95:1069–1073

Shepherd T, Wynne Griffiths D (2006) The effects of stress on plant cuticular waxes. New Phytol 171:469–499

Stimler K, Xing B, Chefetz B (2006) Transformation of plant cuticles in soil: effect on their sorptive capabilities. Soil Sci Soc Am J 70:1101–1109

Sturaro M, Hartings H, Schmelzer E et al (2005) Cloning and characterization of *GLOSSY1*, a maize gene involved in cuticle membrane and wax production. Plant Physiol 138:478–489

Wellesen K, Durst F, Pinot F et al (2001) Functional analysis of the *LACERATA* gene of *Arabidopsis* provides evidence for different roles of fatty acid omega-hydroxylation in development. Proc Natl Acad Sci USA 98:9694–9699

Woo YM, Park HJ, Su'udi M et al (2007) *Constitutively wilted 1*, a member of the rice *YUCCA* gene family, is required for maintaining water homeostasis and an appropriate root to shoot ratio. Plant Mol Biol 65:125–136

Xiao F, Goodwin SM, Xiao Y et al (2004) *Arabidopsis CYP86A2* represses *Pseudomonas syringae* type III genes and is required for cuticle development. EMBO J 23:2903–2913

Xu X, Dietrich CR, Delledonne M et al (1997) Sequence analysis of the cloned *glossy8* gene of maize suggests that it may code for a beta-ketoacyl reductase required for the biosynthesis of cuticular waxes. Plant Physiol 115:501–510

Yoshida R, Hobo T, Ichimura K et al (2002) ABA-activated SnRK2 protein kinase is required for dehydration stress signaling in *Arabidopsis*. Plant Cell Physiol 43:1473–1483

Yu D, Ranathunge K, Huang H et al (2008) Wax *Crystal-Sparse Leaf1* encodes a beta-ketoacyl CoA synthase involved in biosynthesis of cuticular waxes on rice leaf. Planta 228:675–685